

See discussions, stats, and author profiles for this publication at: <https://www.researchgate.net/publication/51557500>

# Influence of the Chemical Structure of Water-Soluble Cryptophanes on Their Overall Chiroptical and Binding Properties

ARTICLE *in* THE JOURNAL OF ORGANIC CHEMISTRY · AUGUST 2011

Impact Factor: 4.72 · DOI: 10.1021/jo201167w · Source: PubMed

CITATIONS

18

READS

18

## 5 AUTHORS, INCLUDING:



**Aude Bouchet**

Technische Universität Berlin

18 PUBLICATIONS 173 CITATIONS

SEE PROFILE



**Mathieu Linares**

Linköping University

63 PUBLICATIONS 983 CITATIONS

SEE PROFILE



**Cavagnat Dominique**

Université Bordeaux 1

73 PUBLICATIONS 1,054 CITATIONS

SEE PROFILE



**Thierry Buffeteau**

Université Bordeaux 1

159 PUBLICATIONS 3,805 CITATIONS

SEE PROFILE

# Influence of the Chemical Structure of Water-Soluble Cryptophanes on Their Overall Chiroptical and Binding Properties

Aude Bouchet,<sup>†</sup> Thierry Brotin,<sup>\*,‡</sup> Mathieu Linares,<sup>#</sup> Dominique Cavagnat,<sup>†</sup> and Thierry Buffeteau<sup>\*,†</sup>

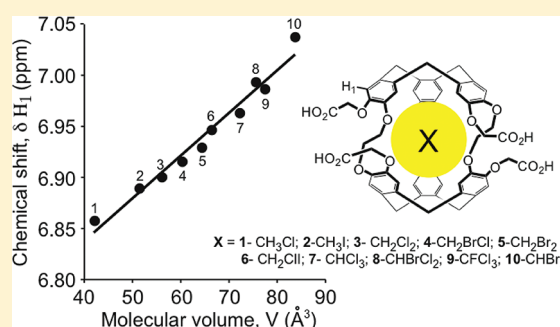
<sup>†</sup>Institut des Sciences Moléculaires (UMR 5255 – CNRS), Université Bordeaux 1, 351 Cours de la Libération, 33405 Talence, France

<sup>‡</sup>Laboratoire de Chimie de l'ENS-LYON (UMR 5182 – CNRS), Ecole Normale Supérieure de Lyon, 46 Allée d'Italie, 69364 Lyon 07, France

<sup>#</sup>Department of Computational Physics, Linköping University, 581 83 Linköping, Sweden

 Supporting Information

**ABSTRACT:** The synthesis and the chiroptical properties of the two enantiomers of the hexacarboxylic acid cryptophane-A derivative, **1**, are described in this article. The chiroptical and binding properties of **1** toward achiral and chiral guests have been investigated in water under basic conditions by polarimetry, electronic circular dichroism (ECD), vibrational circular dichroism (VCD), and <sup>1</sup>H NMR spectroscopy. These experiments reveal that the <sup>1</sup>H NMR spectra of **1** are very sensitive to the nature of the guest trapped in its cavity whereas ECD and VCD spectra remain unchanged. We also show that the two enantiomers of **1** are able to distinguish between the two enantiomers of a series of small chiral epoxides. The enantiodiscrimination increases with the size of the chiral guest whereas the corresponding binding constants decrease. In contrast to what was observed for other water-soluble cryptophanes, the molecular recognition process is found independent of the nature of the counterions surrounding host **1**, shedding light on the importance of the chemical structure of cryptophanes on their binding and chiroptical properties.



## INTRODUCTION

Molecular recognition of neutral achiral or chiral derivatives by supramolecular host molecules is one of the most important topics in today's chemistry and plays an important role in many fields of organic chemistry. Thus, for several decades, chemists have developed various chemical structures able to recognize guest molecules with a high selectivity.<sup>1</sup> Among all the systems described in the literature, host molecules possessing an inner cavity are well suited to bind guests selectively because they can isolate them from their surrounding environment and establish specific interactions that contribute to the stabilization of complexes. Self-assembled systems in solution or synthesis of covalent structures possessing an inner cavity have been the two main strategies used to design these supramolecular hosts. Even though the former strategy has been the topic of numerous works during the last two decades,<sup>1c,f,g</sup> the synthesis of covalent structures is of high interest despite the synthetic difficulties to build these molecules.<sup>1a,b,e,h</sup>

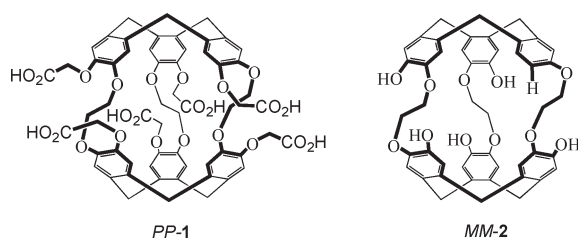
Cryptophane derivatives belong to the second class of compounds. These molecules have attracted a lot of attention since the beginning of the 80s and are still of high interest to bind small neutral atoms or molecules.<sup>1b,h</sup> This feature is the consequence of the tridimensional structure of cryptophanes that creates a lipophilic cavity suitable for accommodating small neutral molecules. The specific molecular recognition is mainly determined

by the internal volume of the cavity that in turn is controlled by the length of the aliphatic linkers (81 Å<sup>3</sup>, 95 Å<sup>3</sup>, and 121 Å<sup>3</sup> for methylenedioxy, ethylenedioxy, and propylenedioxy linkers, respectively) that connect the two cyclotrimeratrylene (CTV) bowls. In addition, some of these host molecules are chiral compounds, and the molecular recognition can be investigated by chiroptical techniques, such as polarimetry, electronic circular dichroism (ECD), and vibrational circular dichroism (VCD).<sup>2</sup> The results obtained by these techniques have revealed that the chiroptical properties of cryptophane-A derivatives are strongly dependent on some external parameters such as the nature of the solvent (organic or aqueous) and the ability of a guest molecule to enter the cavity. Thus, significant and specific ECD responses upon complexation have been observed for water-soluble cryptophane-A that depend on the size of the guest and the nature of the counterion (Li<sup>+</sup>, Na<sup>+</sup>, K<sup>+</sup>, Cs<sup>+</sup>) present in the solution.<sup>2d,e</sup> More importantly, these chiral host molecules are able to achieve enantioselective complexation with small chiral guests. The enantioselective complexation of CHFCIBr and CHFCII molecules by chiral cryptophane-C and enantioenriched cryptophane-E-(SCH<sub>3</sub>)<sub>6</sub>, respectively, are two notable examples reported in the past.<sup>3</sup> Recently, we have shown that the two

Received: June 6, 2011

Published: August 09, 2011

**Scheme 1. Chemical Structure of Water-Soluble Cryptophanes 1 and 2 (only one enantiomer is shown)**



enantiomers of pentahydroxyl cryptophane-A, a water-soluble cryptophane-A congener, are able to discriminate between the two enantiomers of propylene oxide (PrO).<sup>4</sup> This enantiodiscrimination has been clearly demonstrated in water under basic conditions by using either <sup>1</sup>H NMR or ECD spectroscopy and has been found independent of the counterion (Li<sup>+</sup>, Na<sup>+</sup>, K<sup>+</sup>) present in the solution whereas the binding constants associated with the recognition process can be modulated by carefully choosing the nature of the counterion surrounding the host molecule.

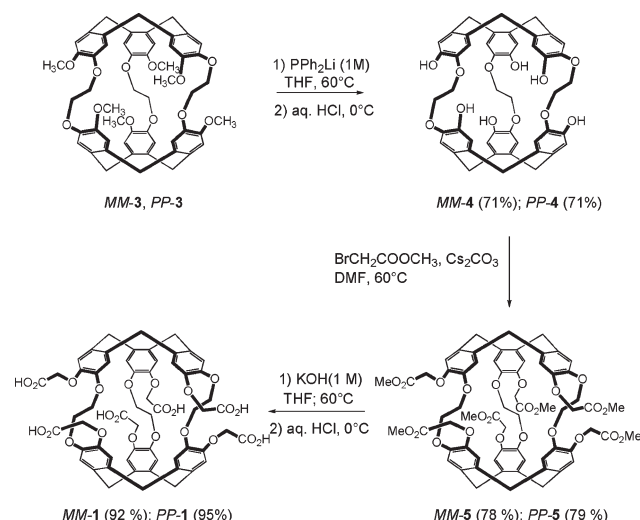
In the light of these results, it is important to determine which factors influence the molecular recognition process for water-soluble cryptophanes. To investigate the effects of electronic and steric factors, the two enantiomers of the hexacarboxylic acid cryptophane-A derivative, **1**, have been synthesized and the chiroptical properties as well as the binding with achiral or chiral guests have been investigated in water under basic conditions. Even though hosts **1** and **2** possess a similar cavity volume, host **1** differs by a higher symmetry and by the replacement of the hydroxyl functions by alkyl arms with terminal carboxylic acid groups. As a consequence, the inner cavity of host **1** is less accessible to guest molecules, and the six counterions are located at a greater distance from the center of the cavity (Scheme 1).

We describe in this article the synthesis of the enantiopure hexacarboxylic acid cryptophane-A, **1**. The chiroptical properties of its two enantiomers MM-**1** and PP-**1** were investigated in water under basic conditions (pH > 12) by polarimetry, electronic circular dichroism, and vibrational circular dichroism. The binding properties of **1** with chiral and achiral guest molecules have been also investigated by <sup>1</sup>H NMR spectroscopy. The effects of the nature of the counterions and the size of the guests on the chiroptical and binding properties of host **1** have been thoroughly studied. Finally, a conformational analysis of MM-**1** has been performed using molecular dynamics (MD) and ab initio calculations at the density functional theory (DFT) level to support experimental VCD results.

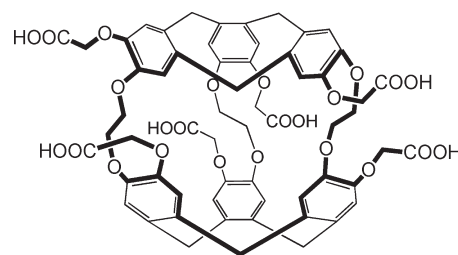
## RESULTS AND DISCUSSION

**Synthesis of Hexacarboxylic Acid Cryptophane-A, 1.** The synthesis of racemic hexacarboxylic acid cryptophane-A, *rac*-**1**, has been previously published in 1987 by Collet and co-workers.<sup>5</sup> The synthetic route used to obtain *rac*-**1** and its two enantiomers MM-**1** and PP-**1** from cryptophane-A *rac*-**3** and its two enantiomers MM-**3** and PP-**3** is presented in Scheme 2. The synthesis of *rac*-**3** is well-known and can now be prepared in fair yield.<sup>6</sup> In addition, the MM-**3** and PP-**3** enantiomers of cryptophane-A have been obtained with excellent enantiomeric excess (ee ≥ 98–99%) by using a procedure developed in 2003.<sup>7</sup> This strategy provides fair quantities of the two enantiomers of cryptophane-A, which can be used for subsequent reactions. Thus, *rac*-**3**, MM-**3**,

**Scheme 2. Synthetic Route Used for the Synthesis of MM-1 and PP-1**



**Scheme 3. Imploded Form of Cryptophane 1**



and PP-**3** were allowed to react with an excess of a solution of freshly prepared lithium diphenylphosphide (1 M) in THF to provide the corresponding hexaphenol derivatives *rac*-**4**, MM-**4**, and PP-**4** derivatives. At this stage, a great care must be taken in the purification of **4**. Compounds **4** were then allowed to react with methyl bromoacetate to provide the corresponding hexaester derivatives *rac*-**5**, MM-**5**, and PP-**5**. It is noteworthy that, according to Prelog's rules, the descriptors *M* and *P* are reversed for the hexaphenol and the hexaester derivatives.<sup>8</sup> Thus, the MM-**4** gives rise to the PP-**5**. In turn the PP-**4** gives rise to the MM-**5** derivative. Hydrolysis of *rac*-**5**, MM-**5**, and PP-**5** under basic conditions followed by acidification with aqueous HCl provides the desired *rac*-**1**, MM-**1**, and PP-**1** derivatives in good yields. The <sup>1</sup>H and <sup>13</sup>C NMR spectra of the PP-**1** enantiomer are reported in Supporting Information (Figure S1).

**"Imploded" Structure of 1.** It has been previously established that the racemic hexacarboxylic acid cryptophane-A derivative can adopt two main conformations ("crown–crown" and "crown–saddle") in basic solution.<sup>9</sup> The presence of the unusual "crown–saddle" conformation is strongly dependent on the purification of the cryptophane **1** derivative and in particular on the presence of a guest molecule inside its cavity. Indeed, in the absence of a guest molecule, one of the two CTV units can collapse to provide the "imploded" structure, such as that depicted in Scheme 3. This particular structure had been previously observed for cryptophanes having longer bridges and consequently a larger inner cavity,<sup>10</sup> but the "imploded" structure of cryptophane-A has been demonstrated only recently

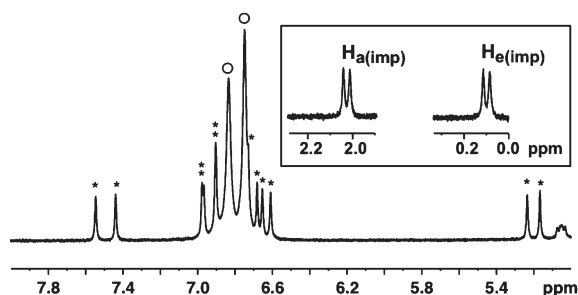


**Figure 1.**  $^1\text{H}$  NMR spectrum (aromatic part) of *rac*-1 showing its globular structure ( $D_3$ -symmetry) and its imploded structure ( $C_1$ -symmetry) in  $\text{D}_2\text{O}/\text{NaOD}$  solution at 293 K. Stars denote aromatic protons of the imploded structure, and circles stand for the two signals corresponding to the globular structure. In insert: high-field shifted protons  $\text{H}_a$  and  $\text{H}_e$  of the methylene bridge pointing toward the center of the cavity. The whole spectrum is given in Supporting Information (Figure S2).

by  $^1\text{H}$  NMR spectroscopy.<sup>9</sup> Since then, this unusual structure has been observed for *rac*-4 and other cryptophane-A congeners.<sup>11</sup>

The imploded form is characterized by a  $C_1$ -symmetry structure, which can be easily observed by  $^1\text{H}$  NMR spectroscopy. Indeed, as shown in Figure 1, the aromatic part of the spectrum reveals 12 additional signals, which are characteristic of the 12 nonequivalent aromatic protons expected for this structure. Two of them are shifted by 1.8 ppm toward the low frequencies. In addition, the two  $\text{H}_a$  (axial) and  $\text{H}_e$  (equatorial) protons of the methylene bridge of the CTV unit are shifted by 3.5 ppm and appear as a pair of doublets at 2.0 ppm and 0.1 ppm, respectively. The presence of these two high shielded protons reveals that they experience the shielding effect of the aromatic rings and that they are present in the inner cavity of **1**, as expected for the imploded structure. This unusual structure can only be obtained in the absence of the guest molecule inside the inner cavity of **1** and is favored upon heating host **1** under vacuum for several hours. Recently, Dmochowski and co-workers obtained an X-ray structure of the imploded form of a cryptophane-A congener.<sup>12</sup> This structure was found in good agreement with the observations deduced from the  $^1\text{H}$  NMR data. Indeed, this X-ray structure clearly shows only one methylene bridge pointing toward the center of the cavity. Several attempts to obtain solely the imploded form in solution failed, and  $^1\text{H}$  NMR spectra recorded for all the studied samples have revealed the presence of the two imploded and globular structures in various proportions. It is noteworthy that the imploded form of host **1** is unable to bind any guest molecules in solution. Thus, this conformer does not compete with the usual globular conformer for the encapsulation of guest molecules, but it complicates the study of the chiroptical and binding properties of host **1** because the proportion of the imploded form present in solution can vary from one sample to another.

**Binding Properties of Achiral Guests.**  $^1\text{H}$  NMR spectroscopy appears as the method of choice to investigate the molecular recognition of host **1** with guest molecules. Encapsulation of small neutral molecules was first investigated with *rac*-1 in water under basic condition. Thus, a series of small tetrahedral molecules  $\text{CH}_3\text{Cl}$  ( $V_{\text{vdw}} = 42.0 \text{ \AA}^3$ ),<sup>13</sup>  $\text{CH}_3\text{I}$  ( $V_{\text{vdw}} = 54.6 \text{ \AA}^3$ ),  $\text{CH}_2\text{Cl}_2$  ( $V_{\text{vdw}} = 56.3 \text{ \AA}^3$ ),  $\text{CH}_2\text{BrCl}$  ( $V_{\text{vdw}} = 60.4 \text{ \AA}^3$ ),  $\text{CH}_2\text{Br}_2$  ( $V_{\text{vdw}} = 64.4 \text{ \AA}^3$ ),  $\text{CHCl}_3$  ( $V_{\text{vdw}} = 71.5 \text{ \AA}^3$ ),  $\text{CHBrCl}_2$  ( $V_{\text{vdw}} = 75.6 \text{ \AA}^3$ ),  $\text{CH}_2\text{I}_2$  ( $V_{\text{vdw}} = 76.4 \text{ \AA}^3$ ),  $\text{CFCl}_3$  ( $V_{\text{vdw}} = 77.6 \text{ \AA}^3$ ), and

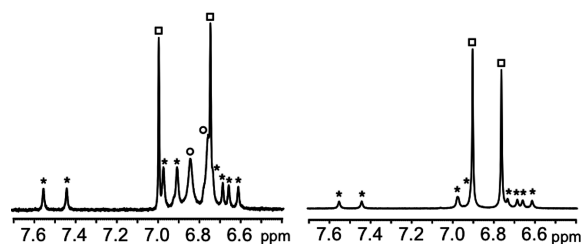


**Figure 2.**  $^1\text{H}$  NMR spectra of *rac*-1 in the presence of  $\text{CFCl}_3$  (left) and  $\text{CH}_3\text{I}$  (right) in  $\text{D}_2\text{O}/\text{NaOD}$  at 293 K. Stars denote aromatic protons of the imploded form. A circle denotes aromatic protons of the guest free form. Squares denote aromatic protons of the filled form.

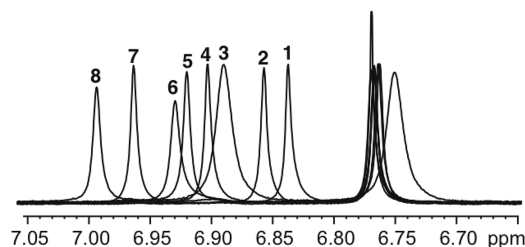


**Figure 3.**  $^1\text{H}$  NMR spectrum of *rac*-1 (aromatic part) in the presence of different guests in  $\text{NaOD}/\text{D}_2\text{O}$  solutions: xenon (1),  $\text{CH}_3\text{Cl}$  (2),  $\text{CH}_3\text{I}$  (3),  $\text{CH}_2\text{Cl}_2$  (4),  $\text{CH}_2\text{BrCl}$  (5),  $\text{CH}_2\text{Br}_2$  (6),  $\text{CHCl}_3$  (7),  $\text{CHBrCl}_2$  (8).

$\text{CCl}_4$  ( $V_{\text{vdw}} = 86.7 \text{ \AA}^3$ ) have been used to test their ability to bind with host **1**. We have observed that for the majority of them (with the exception of  $\text{CCl}_4$  and  $\text{CH}_2\text{I}_2$ ), the  $^1\text{H}$  NMR spectra of **1** are strongly affected by the presence of a guest molecule in its inner cavity. This effect is clearly visible in the aromatic part of the  $^1\text{H}$  NMR spectra of **1**.

Figure 2 shows the  $^1\text{H}$  NMR spectra of **1** in the aromatic part when two guests, exhibiting different van der Waals volumes, are present inside the cavity of **1**. These two spectra reveal that one aromatic proton, initially located at 6.84 ppm for guest-free (hereafter called “empty”) host is deshielded by the presence of a guest molecule. It is noteworthy that the larger the van der Waals volume of the guest, the stronger the deshielding effect. For instance, in the presence of iodomethane, the  $^1\text{H}$  NMR spectrum in the aromatic part appears to be very similar to that observed for empty host **1**, and the two signals corresponding to the aromatic protons of the globular structure appear at 6.89 ppm and 6.76 ppm. In contrast, when iodomethane is replaced by trichlorofluoromethane, these two signals appear at 6.99 and 6.76 ppm. Other investigated tetrahedral guest molecules present a similar behavior. As shown in Figure 3, one of the two aromatic protons of the globular conformer of **1** is highly sensitive to the nature of the guest molecule trapped inside its inner cavity.

The chemical shift modification of one of the aromatic protons observed by  $^1\text{H}$  NMR spectroscopy with host **1** is unique in the series of cryptophane-A congeners. Indeed, this feature had never been observed previously with the cryptophane-A congeners. Like cryptophane-A (with methoxy substituents), host **1** possesses a pseudo  $D_3$ -symmetry, but it differs by the presence of flexible arms with terminal carboxylic acid moieties. These substituents are able to adopt several conformations depending on the nature (and the size) of the guest. In turn, these conformational fluctuations slightly modify the electronic density of the aromatic rings, which may induce a change in the chemical shift of the aromatic proton located in  $\alpha$ -position ( $\delta \text{H}_1$



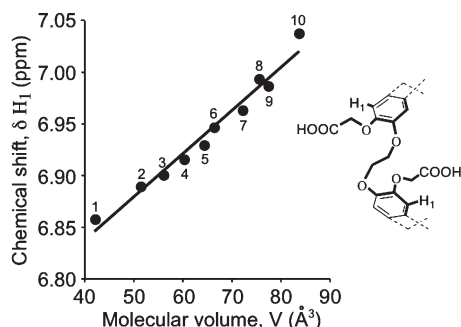


**Figure 4.** Chemical shift (ppm; TMS reference) of the aromatic proton  $H_1$  as a function the guest van der Waals volume.  $^1H$  NMR spectra have been recorded in NaOD (pD = 13.2) at 293 K.  $CH_3Cl$  (1),  $CH_3I$  (2),  $CH_2Cl_2$  (3),  $CH_2BrCl$  (4),  $CH_2Br_2$  (5),  $CH_2ClI$  (6),  $CHCl_3$  (7),  $CHBrCl_2$  (8),  $CFCl_3$  (9),  $CHBr_3$  (10).

in Figure 4). Small molecules such as methane have little influence on  $\delta H_1$  (result not shown) because the van der Waals volume ( $V_{vdw} = 28.4 \text{ \AA}^3$ )<sup>13</sup> represents a small fraction of the cavity (i.e.,  $95 \text{ \AA}^3$ ). Conversely, large guest molecules such as  $CFCl_3$  ( $V_{vdw} = 77.6 \text{ \AA}^3$ ) produce a large shift of  $\delta H_1$  that reflects a strong conformational change in the six arms and the three linkers. Interestingly, as shown in Figure 4, a very good linear relationship can be noticed between the calculated molecular volumes of the guests and the chemical shifts of the aromatic proton  $H_1$ . This result shows that the  $^1H$  NMR spectrum (in the aromatic part) of host **1** is very sensitive to the guest encapsulation process. This feature had not been observed for hexahydroxyl and pentahydroxyl cryptophanes.<sup>2d,e</sup>

It is noteworthy that the same behavior has been observed when sodium cations are replaced by potassium or cesium cations (Supporting Information, Figure S3). A change in the nature of the counterion does not affect the molecular recognition process. In contrast to what was observed with host **2**, the cesium cation does not show any affinity for the cavity of host **1**.

**Binding Properties of Chiral Guests.** We have previously shown that enantiopure water-soluble cryptophane **2** is able to discriminate between the two enantiomers of chiral propylene oxide (PrO,  $V_{dvw} = 57 \text{ \AA}^3$ ).<sup>4</sup> This enantiodiscrimination has been easily detected using either  $^1H$  NMR or ECD spectroscopy. The easy detection of the binding process by  $^1H$  NMR spectroscopy comes from the strong shielding effect of the six aromatic rings surrounding the guest molecule. Thus, the six protons of the bound PrO are located at negative chemical shift values (TMS reference) far away from the usual signals of the free guest and the cryptophane host molecule. We have previously demonstrated that the enantioselective complexation of the two enantiomers of PrO by host **2** occurs and that the binding constants associated with the encapsulation process are strongly dependent on the nature of the counterion ( $Li^+$ ,  $Na^+$ ,  $K^+$ ,  $Cs^+$ ). Because the cavity volumes of hosts **1** and **2** are similar, an enantioselective complexation of small chiral guests can be expected with the two enantiomers *MM-1* and *PP-1*.

In this study, the complexation of several chiral molecules by host **1** has been investigated under various experimental conditions. Figure 5 shows the  $^1H$  NMR spectra of propylene oxide molecule (*rac*-PrO, (*R*)-PrO, and (*S*)-PrO) encapsulated by the *MM-1* enantiomer. Spectra have been recorded at 275 K to reduce the exchange dynamics and to obtain  $^1H$  NMR spectra with a good signal-to-noise ratio. As previously observed with

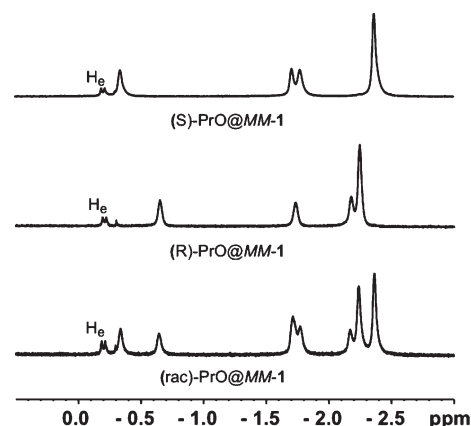


**Figure 5.**  $^1H$  NMR spectra of *MM-1* in the presence of *rac*-PrO, (*R*)-PrO, and (*S*)-PrO in NaOD/ $D_2O$  solution (pD = 13.2) at 275 K.  $H_e$  represents the high-field shifted proton of the methylene bridge pointing toward the center of the cavity in the imploded form of cryptophane **1**.

host **2**, two different spectra are observed for the (*S*)-PrO@*MM-1* and the (*R*)-PrO@*MM-1* complexes. Indeed, the  $^1H$  NMR spectrum of the former displays four distinct signals located at  $-0.32$ ,  $-1.68$ ,  $-1.75$ , and  $-2.35$  ppm, whereas the latter shows four signals located at  $-0.65$ ,  $-1.72$ ,  $-2.18$ , and  $-2.22$  ppm. The  $^1H$  NMR spectrum of *MM-1* in the presence *rac*-PrO shows a combination of all these signals with a preferential affinity for the (*S*)-PrO@*MM-1* diastereomers. Indeed, the relative intensity of the two signals located at  $-0.32$  and  $-0.65$  ppm indicates a small difference in the proportions of (*S*)-PrO@*MM-1* and (*R*)-PrO@*MM-1* diastereomers [(*S*)-PrO@*MM-1*/(*R*)-PrO@*MM-1*  $\approx 1.17$ ]. The enantiodiscrimination is lower than that obtained with host **2**.<sup>4</sup>

A change in the nature of the counterion does not affect the molecular recognition process. For instance, when sodium cations are replaced by cesium cations, the encapsulation of the two enantiomers of the PrO molecule is still clearly visible at 275 K with a small preference for the (*S*)-PrO@*MM-1* diastereomers (Supporting Information, Figure S4).

A similar behavior occurs when propylene oxide is replaced by epichlorohydrin (EPiCl;  $V_{dvw} = 72 \text{ \AA}^3$ ) or 1,2-epoxybutane (1,2-EPoBu;  $V_{dvw} = 78 \text{ \AA}^3$ ). In the case of EPiCl the  $^1H$  NMR spectrum of the (*S*)-EPiCl@*MM-1* diastereomer is very different from that of the (*R*)-EPiCl@*MM-1* diastereomer (Supporting Information, Figure S5). The  $^1H$  NMR spectrum of the *rac*-EPiCl@*MM-1* diastereomer shows a preferential encapsulation for the (*R*)-EPiCl with an enantiodiscrimination better than that for the PrO [(*R*)-EPiCl@*MM-1*/(*S*)-EPiCl@*MM-1*  $\approx 1.4$ ]. As shown in Figure 6, the 1,2-EPoBu guest molecule also enters the cavity of host **1**, but the (*R*)-1,2-EPoBu enantiomer is poorly recognized by *MM-1*. The  $^1H$  NMR spectra of the two diastereomeric complexes are very different, indicating a very high enantiodiscrimination. Indeed, the  $^1H$  NMR spectrum of the (*S*)-1,2-EPoBu@*MM-1* diastereomer reveals five well-resolved signals located at  $-0.3$ ,  $-1.59$ ,  $-1.91$ ,  $-2.42$ , and  $-3.02$  ppm, whereas no distinct signals are detected for the (*R*)-1,2-EPoBu@*MM-1* diastereomer. This result suggests a clear preference for the (*S*)-1,2-EPoBu enantiomer with a strong enantiodiscrimination. Finally, we have observed that the 2,3-epoxybutane (*cis*–*trans* mixture;  $V_{dvw} = 74.2 \text{ \AA}^3$ ) and glycidol ( $V_{vdw} = 65.7 \text{ \AA}^3$ ) do not bind host **1** because no signals were detected at negative chemical shift values for the two enantiomers (spectra not shown).

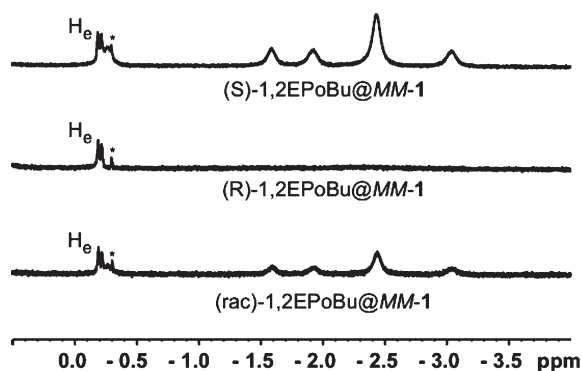


**Figure 6.**  $^1\text{H}$  NMR spectrum of *MM-1* in the presence of *rac*-1,2-EPoBu, (*R*)-1,2-EPoBu, and (*S*)-1,2-EPoBu at 275 K in NaOD (pD = 13.2). The star denotes an impurity in water.

**Table 1.** Binding Constants of *MM-1* and *PP-1* Measured from  $^1\text{H}$  NMR Spectra in Presence of (*R*)- and (*S*)-PrO, (*R*)- and (*S*)-EPiCl, and (*R*)- and (*S*)-1,2-EPoBu<sup>a</sup>

diastereomer	Soln	host concn (mM)	$V_{\text{guest}}$ ( $\text{\AA}^3$ )	$K$ ( $\text{M}^{-1}$ ) <sup>b</sup>
( <i>R</i> )-PrO@ <i>PP-1</i>	NaOD/D <sub>2</sub> O	7.0	57	128
( <i>S</i> )-PrO@ <i>PP-1</i>	NaOD/D <sub>2</sub> O	7.1	57	99
( <i>R</i> )-PrO@ <i>MM-1</i>	CsOD/D <sub>2</sub> O	7.9	57	86
( <i>S</i> )-PrO@ <i>MM-1</i>	CsOD/D <sub>2</sub> O	15.8	57	126
( <i>R</i> )-EPiCl@ <i>MM-1</i>	NaOD/D <sub>2</sub> O	17.4	72	64
( <i>S</i> )-EPiCl@ <i>MM-1</i>	NaOD/D <sub>2</sub> O	19.3	72	47
( <i>R</i> )-1,2EPoBu@ <i>MM-1</i>	NaOD/D <sub>2</sub> O	7.8	78	— <sup>c</sup>
( <i>S</i> )-1,2EPoBu@ <i>MM-1</i>	NaOD/D <sub>2</sub> O	8.1	78	11

<sup>a</sup> Spectra have been measured at 275 K in NaOD/D<sub>2</sub>O or CsOD/D<sub>2</sub>O solutions. <sup>b</sup> Experimental error on  $K$  determination is estimated to be 25%. <sup>c</sup> Could not be measured with precision.

It is noteworthy that the binding properties of host **1** are significantly different from those observed for host **2**. First, the complexes formed with **1** are weaker than those formed with **2**. Indeed, binding constants of  $128 \pm 32 \text{ M}^{-1}$  and  $99 \pm 25 \text{ M}^{-1}$  have been calculated from the  $^1\text{H}$  NMR spectra (Supporting Information, Figures S6 and S7) for the (*R*)-PrO@*PP-1* and (*S*)-PrO@*PP-1* diastereomers, respectively (Table 1). These values are smaller than those determined with host **2** ( $281 \text{ M}^{-1}$  and  $131 \text{ M}^{-1}$  for (*R*)-PrO@*PP-2* and (*S*)-PrO@*PP-2* diastereomers, respectively) under the same experimental conditions (NaOD/D<sub>2</sub>O solutions). In addition, we notice that when the guest size increases, the binding constants strongly decrease (Supporting Information, Figure S8–S11). For instance, binding constants of  $47 \pm 12 \text{ M}^{-1}$  and  $11 \pm 3 \text{ M}^{-1}$  have been found for the (*S*)-EPiCl@*MM-1* and (*S*)-1,2-EPoBu@*MM-1* diastereomers, respectively (Table 1). Secondly, the enantiodiscrimination of PrO by host **1** is significantly lower than that previously observed with host **2**. For instance, *MM-1* recognizes preferentially the (*S*)-PrO enantiomer with a ratio of 1.17, whereas a better enantiodiscrimination was found for host **2** [(*S*)-PrO@*MM-1*/(*R*)-PrO@*MM-1*  $\approx 2.45$ ]. By contrast, the larger the guest molecule within the cavity of host **1**, the greater the enantiodiscrimination effect. Moreover, we notice that the increase of the enantioselective complexation process is associated with the decrease of the binding constants. Thus, the enantiodiscrimination is better with epichlorohydrin and excellent with 1,2-epoxybutane. Finally, the

binding properties of PrO by host **1** are not affected by the nature of counterions (similar values have been obtained in the presence of cesium cations) in contrast to host **2** which shows a high affinity for cesium cations.<sup>4</sup>

**Chiroptical Properties of 1.** Polarimetric measurements of hexacarboxylic acid cryptophane-A **1** have been measured in various solvents and are reported in Table 2. Compound **1** shows in organic solvents (DMF, DMSO) lower optical rotation values than those measured in water under basic conditions, and the two enantiomers *MM-1* and *PP-1* present similar optical rotation values with opposite signs. A slight increase of the magnitude of the measured rotatory power has been observed in NaOH/H<sub>2</sub>O solution upon encapsulation of CH<sub>2</sub>Cl<sub>2</sub> and CHCl<sub>3</sub> guest molecules.

The ECD spectra of *MM-1* and *PP-1* have been measured in the 220–360 nm spectral range by varying the nature of the guest molecules (achiral or chiral molecules) and the nature of the counterions surrounding cryptophane **1**. The ECD spectra of *MM-1* and *PP-1* exhibit a perfect mirror image, but for clarity only one enantiomer is shown in the Figure 7. The ECD spectrum of empty *MM-1* recorded in NaOH/H<sub>2</sub>O solution (0.1 M) exhibits three positive bands located at 296, 276, and 250 nm and one negative band located at 235 nm. Figure 7 shows that the ECD spectrum of empty *MM-1* is little changed by the presence of achiral guest molecules (CH<sub>2</sub>Cl<sub>2</sub>, CHCl<sub>3</sub>). Moreover, the replacement of CH<sub>2</sub>Cl<sub>2</sub> by a CHCl<sub>3</sub> molecule only produces a very small shift of the CD bands. Surprisingly, the presence of the imploded form does not modify significantly the overall ECD spectrum of **1**. Indeed, the ECD spectrum of *MM-1* containing 20–25% of imploded form (as evaluated by  $^1\text{H}$  NMR spectroscopy) leads to very similar ECD spectra in the presence of CH<sub>2</sub>Cl<sub>2</sub> or CHCl<sub>3</sub> guest molecules (Supporting Information, Figure S12). Finally, the ECD spectra of *MM-1* does not allow the distinction between the two enantiomers of a chiral molecule. For instance, the ECD spectra of *MM-1* in the presence of (*R*)-PrO and (*S*)-PrO remain unchanged (Supporting Information, Figure S13).

The ECD spectra of *MM-1* (or *PP-1*) in NaOH/H<sub>2</sub>O solution are almost insensitive to the presence of CH<sub>2</sub>Cl<sub>2</sub> or CHCl<sub>3</sub> molecule in the cavity, whereas *MM-2* and *PP-2* are found very sensitive to guest encapsulation in LiOH/H<sub>2</sub>O and NaOH/H<sub>2</sub>O solutions.<sup>2c</sup> This behavior difference between **1** and **2** shows that the chemical structure of water-soluble cryptophane may affect their chiroptical properties. The presence of phenolate groups under basic condition induces strong modifications in the overall ECD spectra of cryptophane derivatives.<sup>2,de</sup> In contrast, when the charges are far away from the aromatic rings (host **1**) or when cryptophane-A derivatives are investigated in organic solvents,<sup>2a–c</sup> the spectral modifications under encapsulation are very small. The presence of five phenolate groups for host **2** induces certainly a larger deviation of the electronic transition moment, especially for the  $^1\text{L}_b$  and  $^1\text{B}_b$  transitions. Consequently, the ECD spectra of **2** appear more sensitive to conformational changes induced by guest encapsulation<sup>2c</sup> or the presence of the two enantiomers of a chiral molecule.<sup>4</sup> The presence of phenolate also increases the electronic density of the aromatic rings and leaves the cavity more nucleophilic. This effect may explain why host **2** is able to encapsulate cations such as cesium under basic conditions.

The chiroptical properties of enantiopure cryptophane **1** have been also investigated by vibrational circular dichroism. IR and VCD experiments of empty *MM-1* as well as *MM-1* in the presence of CD<sub>2</sub>Cl<sub>2</sub> and CDCl<sub>3</sub> have been performed in NaOD/D<sub>2</sub>O solution ([NaOD] = 0.21 M). The corresponding IR and VCD spectra are reported in the 1800–1250 cm<sup>−1</sup> spectral

**Table 2.** Optical Rotations  $[\alpha]_D^{25}$  ( $10^{-1}$  deg cm<sup>2</sup> g<sup>-1</sup>) of *MM-1* and *PP-1* in DMF, DMSO, and NaOH/H<sub>2</sub>O (0.1 M) at 25 °C (experimental errors are estimated to  $\pm 5\%$ )

compd	solvent	concn <sup>a</sup>	$[\alpha]_D^{25}$ <sub>589</sub>	$[\alpha]_D^{25}$ <sub>577</sub>	$[\alpha]_D^{25}$ <sub>546</sub>	$[\alpha]_D^{25}$ <sub>436</sub>	$[\alpha]_D^{25}$ <sub>365</sub>
<i>MM-1</i>	DMF	0.20	+187.3	+197.0	+229.1	+437.7	+849.5
<i>PP-1</i>	DMF	0.14	-188.4	-198.6	-232.6	-438.3	-827.4
<i>PP-1</i>	DMSO	0.22	-205.2	-213.2	-253.9	-470.3	-878.6
<i>MM-1</i>	NaOH/H <sub>2</sub> O	0.18	+279.5	+294.1	+340.7	+649.8	+1278.4
<i>PP-1</i>	NaOH/H <sub>2</sub> O	0.11	-278.7	-293.8	-339.1	-637.8	-1196.2
CH <sub>2</sub> Cl <sub>2</sub> @ <i>PP-1</i>	NaOH/H <sub>2</sub> O	0.27	-305.2	-320.0	-369.3	-696.5	-1305.1
CHCl <sub>3</sub> @ <i>PP-1</i>	NaOH/H <sub>2</sub> O	0.11	-328.7	-345.2	-399.0	-742.5	-1393.3
CHCl <sub>3</sub> @ <i>MM-1</i>	NaOH/H <sub>2</sub> O	0.28	+329.2	+346.6	+401.3	+753.5	+1410.4

<sup>a</sup> Concentration is given in grams per 100 mL.

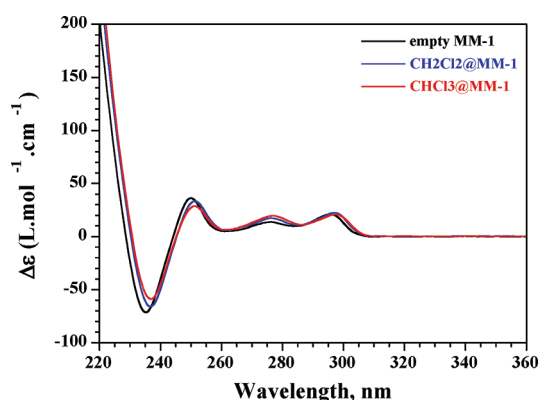


**Figure 7.** ECD spectra of empty *MM-1* (black spectrum) as well as *MM-1* in the presence of CH<sub>2</sub>Cl<sub>2</sub> (blue spectrum) and CHCl<sub>3</sub> (red spectrum) in NaOH/H<sub>2</sub>O (0.1 M) solution at 293 K.

range in Figure 8a and 8b, respectively. Samples of *MM-1* have been prepared at a concentration of 0.03 M to provide VCD spectra with a sufficient signal-to-noise ratio. The IR and VCD spectra of empty *MM-1* in DMSO-*d*<sub>6</sub> are also reported in Figures 8 to obtain vibrational information of cryptophane **1** with the carboxylic acid form. Most of the bands observed in the IR spectrum of empty *MM-1* in DMSO-*d*<sub>6</sub> have been previously assigned for other cryptophane-A derivatives,<sup>2a-c</sup> except the band associated with the  $\nu$ C=O stretching vibration of the carboxylic acid groups which appears at 1736 cm<sup>-1</sup>. The bands due to the  $\nu_{8a}$ C=C,  $\nu_{8b}$ C=C, and  $\nu_{19a}$ C=C stretching vibrations of the rings occur at 1607, 1576, and 1509 cm<sup>-1</sup>, respectively. The bending vibration of CH<sub>2</sub> groups gives rise to the band observed at 1444 cm<sup>-1</sup>. The region between 1400 and 1250 cm<sup>-1</sup> is more complex because the observed bands correspond to coupled modes involving wagging and twisting vibrations of the CH<sub>2</sub> groups (chains and bowls). The VCD spectrum of empty *MM-1* in DMSO-*d*<sub>6</sub> is very similar in shape and intensity to that reported for (+)-cryptophane-A derivative in organic solvents.<sup>2a</sup> Thus, the replacement of the six methoxy groups by a OCH<sub>2</sub>COOH moiety does not significantly change the VCD spectrum of cryptophane-A derivatives. The similar electron-donating character of the two substituents does not alter the electronic circulation in the CTV units and, consequently, does not significantly change the VCD band intensities. Finally, the  $\nu$ C=O stretching vibration gives rise to a very weak positive VCD band around 1740 cm<sup>-1</sup>.

The IR spectrum of empty *MM-1* in NaOD/D<sub>2</sub>O solution exhibits significant spectral modifications in the 1800–1250 cm<sup>-1</sup>

spectral range, because carboxylate groups replace the carboxylic acid groups at basic pH. Consequently, the band located at 1736 cm<sup>-1</sup> in DMSO-*d*<sub>6</sub> disappears and gives rise to the bands located at 1606 and 1423 cm<sup>-1</sup>, associated with the asymmetric ( $\nu_a$ COO<sup>-</sup>) and symmetric ( $\nu_s$ COO<sup>-</sup>) stretching vibrations of the carboxylate groups, respectively. It is noteworthy that the integrated intensity of the  $\nu_a$ COO<sup>-</sup> band is about three times higher than that of the  $\nu$ C=O band for the carboxylic acid form. The VCD spectrum of empty *MM-1* in NaOD/D<sub>2</sub>O solution is significantly different from that recorded in DMSO-*d*<sub>6</sub>, except the  $\nu$ C=C band at 1509 cm<sup>-1</sup> which remains the most intense VCD band with a positive sign. This VCD spectrum exhibits a strong negative couplet (positive at higher frequency and negative at lower frequency) for the  $\nu_a$ COO<sup>-</sup> mode. This bisignate band arises from the coupling of a pair of oriented dipoles and can be easily interpreted using the degenerate coupled oscillator (DCO) model,<sup>15</sup> which is particularly well adapted to interpret the VCD spectra of dimeric molecules.<sup>16</sup> The sign and the intensity of this couplet are strongly dependent on the distance and the orientation of  $\nu_a$ COO<sup>-</sup> dipoles and, consequently, can be used to obtain pertinent information about the conformation of the OCH<sub>2</sub>COO<sup>-</sup> moiety. As shown in Figure 8b, the VCD spectrum of empty *MM-1* is not modified by the presence of a CD<sub>2</sub>Cl<sub>2</sub> or CDCl<sub>3</sub> molecule inside the cavity of *MM-1*. Encapsulation of guest molecules by *MM-1* induces no significant effects on the VCD spectra as observed previously on ECD spectra. The complexation of guest molecules is certainly less efficient for host **1** because of the presence of the OCH<sub>2</sub>COO<sup>-</sup> groups. Indeed, intramolecular interactions may occur between two COO<sup>-</sup> (or COOH) groups coming from opposite CTV units and associated with two different linkers, hindering the entrances to the cryptophane cavity.

**Conformational Analysis of 1.** The average conformation of host **1** and its eventual modification upon encapsulation have been determined from molecular mechanics (MM) and molecular dynamics (MD) calculations. These calculations were performed for the carboxylic acid (in DMSO) and the carboxylate forms (in water with Na<sup>+</sup> and Cs<sup>+</sup> as counterions) of empty *MM-1* and the CHCl<sub>3</sub>@*MM-1* complex. Two parameters have been followed during the dynamics: the dihedral angles of the three OCH<sub>2</sub>CH<sub>2</sub>O linkers (values around  $\pm 60^\circ$  and  $\pm 180^\circ$  reveal gauche and trans conformations of the linkers, respectively) and the three distances between the nearest COOH (or COO<sup>-</sup>) groups. We have also followed the distances of each sodium and cesium cation with respect to the center of cryptophane cavity to investigate the potentiality of **1** to complex cations.



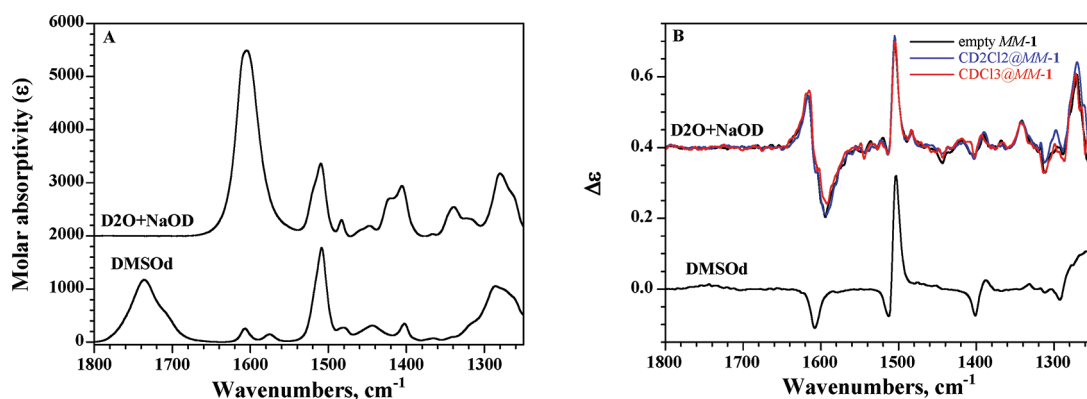


**Figure 8.** (A) IR spectra of empty *MM-1* in DMSO-*d*<sub>6</sub> (bottom) and in D<sub>2</sub>O/NaOD (0.21 M) solution (top). (B) VCD spectra of empty *MM-1* in DMSO-*d*<sub>6</sub> (bottom) and in D<sub>2</sub>O/NaOD (0.21 M) solution (top, black). VCD spectra of *MM-1* in the presence of CD<sub>2</sub>Cl<sub>2</sub> (top, blue) and CDCl<sub>3</sub> (top, red) are also reported.

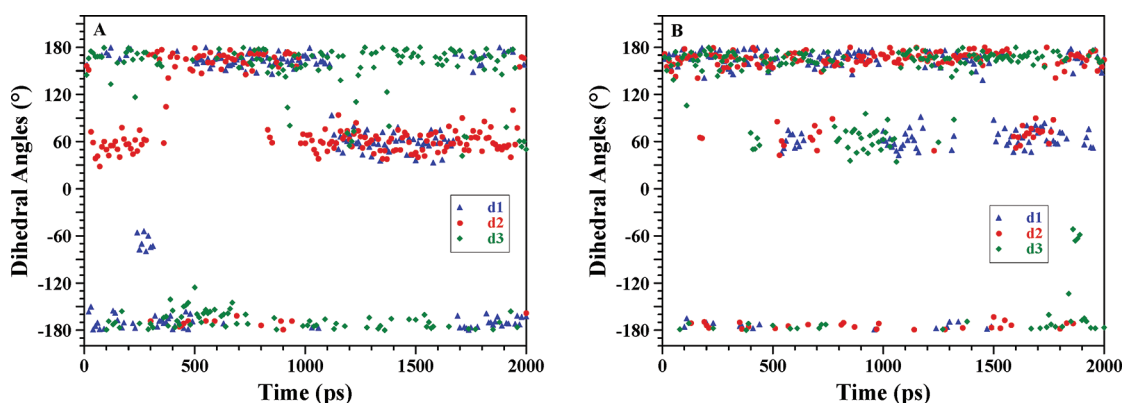


**Figure 9.** Dihedral angles of the three linkers during 2 ns of the dynamics. These values have been extracted from the MD calculations for the carboxylate form with Na<sup>+</sup> counterions of (A) empty *MM-1* and (B) CHCl<sub>3</sub>@*MM-1* complex.

As shown in Figure 9, empty *MM-1* favors the TTG conformation (66% T – 34% G)<sup>17</sup> of the linkers in water with Na<sup>+</sup> counterions. The MD calculations performed for the CHCl<sub>3</sub>@*MM-1* complex reveal a higher proportion of trans conformation of the linkers (78% T / 22% G). A similar behavior had been previously observed for the pentahydroxyl cryptophane-A derivative.<sup>2e</sup> The calculations performed with Cs<sup>+</sup> counterions (Supporting Information, Figure S14) slightly increase the conformational changes upon encapsulation (59% T/41% G for empty *MM-1* versus 81% T/19% G for CHCl<sub>3</sub>@*MM-1* complex). The distances between the counterions (sodium or cesium) and the center of the cavity are presented in Supporting Information (Figure S15). For sodium counterions, these distances are higher than those calculated for cryptophane **2**. Moreover, our MD calculations show that the cesium cations are not able to enter the cavity of *MM-1*, in contrast to that observed for host **2**.<sup>2e</sup> This last result is due to the fact the cavity of **1** is less nucleophilic than that of **2** (the phenolate groups for **2** increase the electronic density of the aromatic rings). We have mentioned in the previous paragraph that the complexation of guest molecules is certainly less efficient for host **1** because of the presence of intramolecular interactions between the OCH<sub>2</sub>COO<sup>−</sup> groups coming from opposite CTV units and associated with two different linkers. The three nearest distances between two carboxylate groups have been determined from the MD calculations (Supporting Information, Figure S16). The average values of these distances (i.e., 4.54 Å, 4.67 Å, and 6.43 Å) confirm the intramolecular

interactions between the OCH<sub>2</sub>COO<sup>−</sup> groups. These distances can also explain the oscillator coupling observed on the VCD spectrum for the ν<sub>a</sub>COO<sup>−</sup> mode. However, the high intensity of the observed negative couplet is due to the strong oscillator strength of the ν<sub>a</sub>COO<sup>−</sup> mode.

To confirm our conformational analysis of **1**, ab initio calculations at the density functional theory (DFT) level have been performed for the carboxylic acid and carboxylate forms by using the geometries of empty *MM-1* obtained from MD simulations. These geometries were optimized at the B3PW91/6-31G\* level, and harmonic vibrational frequencies were calculated at the same level. The calculated VCD spectrum of the carboxylate form of *MM-1* is reported in Figure 10 for comparison with the experimental VCD spectrum of empty *MM-1* recorded in D<sub>2</sub>O/NaOD solution. A good agreement is observed between the calculated and experimental spectra, indicating that the average conformation of the linkers extracted from the MD simulations is representative of the investigated system. The experimental VCD spectrum of empty *MM-1* in DMSO-*d*<sub>6</sub> is also well reproduced by the DFT spectrum calculated for its carboxylic acid form (Supporting Information, Figure S17).

## CONCLUSION

In this article we have described the synthesis of the two enantiomers of a hexacarboxylic acid cryptophane-A derivative **1**.



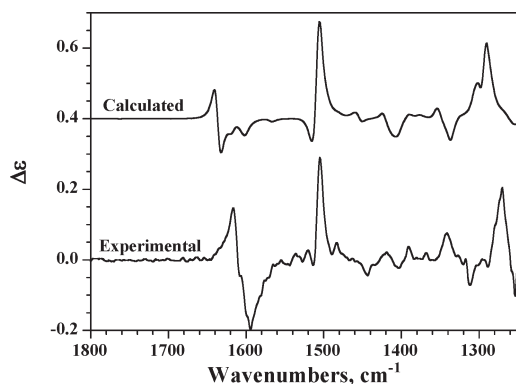


**Figure 10.** Comparison of the experimental VCD spectrum of empty *MM*-1 recorded in  $D_2O/NaOD$  solution (0.21 M) with the calculated spectrum at the B3PW91/6-31G\* level for the carboxylate form of *MM*-1.

We have shown that compound **1** may present two different structures: the globular form which is the most usual structure of cryptophane-A derivatives, and the imploded form which is less common, because it is usually observed only for large cryptophanes. The chiroptical and binding properties of the globular form of **1** have been extensively studied by polarimetry, ECD, VCD, and  $^1H$  NMR spectroscopy and are found significantly different from those recently published for pentahydroxyl cryptophane-A derivative **2**. This article sheds light on the importance of the chemical structure of cryptophanes on their binding and chiroptical properties. For instance, we conclude that the presence of the phenolate groups (in basic solution) for compound **2** plays a key role in the chiroptical (in particular ECD) changes observed with achiral or chiral guest molecules. In addition, the higher electronic density of the aromatic rings for compound **2** increases the nucleophilic character of its cavity that enables host **2** to bind ionic species such as cesium cations. In contrast, no significant ECD and VCD modifications have been observed upon encapsulation for compound **1**, under the same experimental conditions. A less efficient complexation of guest molecules by host **1** because of steric hindrance from the peripheral substituents may explain this behavior. Moreover, the remoteness of the negative charges for compound **1** decreases the nucleophilic character of the cavity, preventing the binding of cations. On the other hand, the  $^1H$  NMR spectra of host **1** are more sensitive to encapsulation effects than the  $^1H$  NMR spectra of host **2**, and they are very specific to the size of the guests. Finally, we have shown that *MM*-1 and *PP*-1 are able to discriminate between the two enantiomers of propylene oxide, epichlorohydrin, and 1,2-epoxybutane. This enantiodiscrimination increases with the size of the guest molecule whereas the corresponding binding constants decrease.

## EXPERIMENTAL SECTION

### NMR Spectroscopy, Polarimetric, and ECD Measurements.

$^1H$  NMR spectra were recorded at 500 MHz using a 5-mm liquid probe. Optical rotations of *MM*-1 *PP*-1, were measured at several wavelengths on a polarimeter with a 100 mm cell thermostatted at 25 °C. ECD spectra were recorded at room temperature with a 0.2 cm path length quartz cell. The concentration of *MM*-1 and *PP*-1 used was in the range  $5 \times 10^{-5}$  M to  $10^{-4}$  M in basic  $H_2O$  solution (0.1 M solutions of LiOH, NaOH, KOH, and CsOH). Saturated solutions of various halomethanes in water have been used to study encapsulation of achiral guest molecules. Spectra were

recorded in the 220–400 nm wavelength range with a 0.5 nm increment and a 1 s integration time. Spectra were processed with standard spectrometer software, baseline corrected, and slightly smoothed by using a third-order least-squares polynomial fit. Spectral units were expressed in molar ellipticity.

**IR and VCD Measurements.** The infrared and VCD spectra were recorded with a FTIR spectrometer equipped with a VCD optical bench.<sup>18</sup> IR absorption and VCD spectra were recorded at a resolution of  $4\text{ cm}^{-1}$ , by coadding 50 scans and 24 000 scans (8 h acquisition time), respectively. Samples were held in a  $CaF_2$  cell with a fixed path length of  $45\text{ }\mu\text{m}$ . IR and VCD spectra of *MM*-1 were measured in basic  $D_2O$  (0.21 M solutions of NaOD) and  $DMSO-d_6$  solutions at a concentration of 0.030 M. Baseline corrections of the VCD spectra were performed by subtracting the two opposite-enantiomer VCD spectra of **1** (recorded under the same experimental conditions) with division by two. In all experiments, the photoelastic modulator was adjusted for a maximum efficiency at  $1400\text{ cm}^{-1}$ . Calculations were done with the standard spectrometer software, using Happ and Genzel apodization, de-Haseth phase-correction, and a zero-filling factor of 1. Calibration spectra were recorded using a birefringent plate (CdSe) and a second  $BaF_2$  wire grid polarizer, following the experimental procedure previously published.<sup>19</sup> Finally, in the presented IR spectra, the solvent absorption was subtracted out.

**MM and MD Calculations.** Molecular mechanics (MM) and molecular dynamics (MD) calculations have been performed with the Tinker package<sup>20</sup> and the OPLS force-field<sup>21</sup> in a periodic box big enough to avoid self-interaction problems. For the water molecules, we used the TIP3P model embedded in the OPLS force-field. We applied a cutoff of 10 Å for both electrostatic and van der Waals interactions. The solute has been soaked in a cubic box of water (DMSO) with a size of 27.9 Å (29.4 Å) containing 729 (216) molecules. Given the cutoff of 10 Å, this simulation box is large enough to avoid self-interaction between the cryptophane and its images. The process to dissolve the cryptophane in water (in DMSO) was performed by placing the molecule into the simulation box of a thermally equilibrated water (DMSO) at a concentration of  $1\text{ g/cm}^3$  ( $1.1\text{ g/cm}^3$ ) and by subsequent removal of solvent molecules overlapping with the cryptophane. MD calculations have been performed in the canonical ensemble (NVT) at 300 K using the Berendsen thermostat,<sup>22</sup> with trans conformation of the three linkers as the starting point. During the 2 ns of the dynamics, the values of the dihedral angles of the linkers were recorded every 10 ps.

**DFT Calculations.** The geometry optimizations, vibrational frequencies, and absorption intensities were calculated by Gaussian 03 program<sup>23</sup> on the CIS-IBM (with 16 processors) at the M3PEC computing center of the University Bordeaux I. Calculations of the optimized geometry of empty *MM*-1 and  $CHCl_3@MM$ -1 complex were performed at the density functional theory level using B3PW91 functional and 6-31G\* basis set. The theoretical framework for geometry optimization of cryptophane molecules has been previously published.<sup>2a</sup> Because experiments were performed in DMSO and in water under basic conditions, DFT calculations were performed considering the carboxylic acid ( $OCH_2COOH$  peripheral substituents) and carboxylate ( $OCH_2COO^- Na^+$  peripheral substituents) forms of the molecule with the GTT conformations of the three linkers. Vibrational frequencies and IR intensities were calculated at the same level of theory. For comparison to experiment, the calculated frequencies were scaled by 0.968 and the calculated intensities were converted to Lorentzian bands with a half-width of  $7\text{ cm}^{-1}$ .

**Synthesis.** The synthesis of the two enantiomers *MM*-4 and *PP*-4 has been previously reported.<sup>2d</sup> From these two enantiomers, the synthesis of *PP*-5 and *MM*-5 has been carried out using an experimental procedure previously reported for the racemic compound.<sup>9</sup> Similarly, the *PP*-1 and the *MM*-1 enantiomers have been obtained from *PP*-5 and *MM*-5, respectively, by hydrolysis under basic conditions followed

by acidification with a concd HCl solution. As an example, the two experimental procedures are reported for the MM-5 and MM-1 enantiomers.

**Synthesis of Cryptophane MM-5.** Methyl bromoacetate (0.56 mL, 6 mmol) was added in one portion to a stirred solution of PP-4 (0.2 g, 0.25 mmol) and cesium carbonate (0.48 g, 1.48 mmol) in freshly distilled DMF (4 mL). The mixture was stirred overnight at 80 °C under an argon atmosphere. The mixture was then poured into water, and the product was extracted three times with CH<sub>2</sub>Cl<sub>2</sub>. The combined CH<sub>2</sub>Cl<sub>2</sub> layers were then washed four times with brine and dried over sodium sulfate. Filtration followed by evaporation of the solvent under reduced pressure left a residue, which was then purified on silica gel (CH<sub>2</sub>Cl<sub>2</sub>/acetone: 90/10). Evaporation of the solvent afforded a white solid, which was then recrystallized in CHCl<sub>3</sub>/EtOH. The crystals obtained by filtration on a frit were washed several times with diethyl ether and dried in air. White crystals (0.24 g, 0.19 mmol; 78%) of MM-5 have been obtained from this procedure. Similarly, PP-5 (0.24 g, 0.19 mmol; 78%) has been obtained from MM-4 (0.2 g, 0.25 mmol). <sup>1</sup>H NMR data of MM-5 and PP-5 are identical to those previously reported for *rac*-5.<sup>9</sup>

**Synthesis of Cryptophane MM-1.** A solution of KOH/H<sub>2</sub>O (1M; 7 mL) was added in one portion to a stirred solution of MM-5 (0.21 g, 0.17 mmol) in THF (7 mL). The mixture was stirred overnight at 60 °C under an argon atmosphere. The THF was removed under reduced pressure, and 5 mL of distilled water was added. Acidification with concd HCl at 0 °C afforded a white precipitate, which was collected on a frit. The solid was washed with distilled water and then with diethyl ether to give MM-1 as a white solid (0.18 g, 0.16 mmol; 92%). Similarly, PP-1 (0.17 g, 0.15 mmol; 91%) was obtained from PP-5 (0.2 g, 0.16 mmol). <sup>1</sup>H NMR (500 MHz, DMSO-*d*<sub>6</sub>, 25 °C): δ 6.94 (s, 6H; Ar), 6.90 (s, 6H; Ar), 4.68 (s, 12H; CH<sub>2</sub>), 4.63 (d, 6H, <sup>2</sup>J(H,H) = 13.5 Hz; H<sub>a</sub>), 4.34 (m, 12H; CH<sub>2</sub>), 3.41 (d, 6H, <sup>2</sup>J(H,H) = 13.5 Hz; H<sub>e</sub>). <sup>13</sup>C NMR (125.7 MHz, DMSO-*d*<sub>6</sub>, 25 °C): δ 170.1, 147.0, 145.8, 133.1, 132.7, 119.7, 117.0, 68.3, 66.1, 34.8. Cryptophane MM-1: elemental analysis calcd (%) for C<sub>60</sub>H<sub>54</sub>O<sub>24</sub>, 5 H<sub>2</sub>O: C 57.7, H 5.2, found C 58.1, H 5.0. HRMS (ESI) *m/z* calcd for C<sub>60</sub>H<sub>54</sub>O<sub>24</sub>Na (M<sup>+</sup>) 1181.2897, found 1181.2844. Cryptophane PP-1: elemental analysis calcd (%) for C<sub>60</sub>H<sub>54</sub>O<sub>24</sub>, 5 H<sub>2</sub>O: C 57.7, H 5.2, found C 57.6, H 5.0. HRMS (ESI) *m/z* calcd for C<sub>60</sub>H<sub>54</sub>O<sub>24</sub>Na (M<sup>+</sup>) 1181.2897, found 1181.2850. <sup>1</sup>H and <sup>13</sup>C NMR spectra of the globular conformer of MM-1 and PP-1 are similar to those previously reported for *rac*-1.

## ■ ASSOCIATED CONTENT

**Supporting Information.** <sup>1</sup>H and <sup>13</sup>C NMR spectra of PP-1 in DMSO-*d*<sub>6</sub> solution. <sup>1</sup>H NMR spectra of PP-1 in CsOD/D<sub>2</sub>O solution at 293 K in the presence of CH<sub>2</sub>Cl<sub>2</sub>, CHBrCl<sub>2</sub>, and CHBr<sub>3</sub>. <sup>1</sup>H NMR spectra of MM-1 in D<sub>2</sub>O/NaOD in the presence of (R)-PrO and (S)-PrO. <sup>1</sup>H NMR spectra of MM-1 in D<sub>2</sub>O/CsOD in the presence of *rac*-PrO, (R)-PrO, and (S)-PrO. <sup>1</sup>H NMR spectra of MM-1 in D<sub>2</sub>O/NaOD in the presence of *rac*-EPiCl, (R)-EPiCl, and (S)-EPiCl. <sup>1</sup>H NMR spectra of MM-1 in D<sub>2</sub>O/NaOD in the presence of (R)-1,2-EPoBu and (S)-1,2-EPoBu. ECD spectra of empty MM-1 containing 20–25% of the imploded form as well as MM-1 in the presence of CH<sub>2</sub>Cl<sub>2</sub> and CHCl<sub>3</sub> in NaOH/H<sub>2</sub>O. ECD spectra of MM-1 in the presence of (R)-PrO and (S)-PrO in H<sub>2</sub>O/NaOH solution. MD and DFT calculations. Full list of authors for ref 23. This material is available free of charge via the Internet at <http://pubs.acs.org>.

## ■ AUTHOR INFORMATION

### Corresponding Author

\*E-mail: [t.buffeteau@ism.u-bordeaux1.fr](mailto:t.buffeteau@ism.u-bordeaux1.fr); [thierry.brotin@ens-lyon.fr](mailto:thierry.brotin@ens-lyon.fr).

## ■ ACKNOWLEDGMENT

The authors are indebted to the CNRS (Chemistry Department) and to Région Aquitaine for financial support for FTIR and optical equipment. The authors also acknowledge computational facilities provided by the Pôle Modélisation of the Institut des Sciences Moléculaires and the M3PEC-Mésocentre of the University Bordeaux 1 (<http://www.m3pec.u-bordeaux1.fr>), financed by the Conseil Régional d'Aquitaine and the French Ministry of Research and Technology. Finally, support from the French Ministry of Research (ANR project NT09-472096 GHOST) is acknowledged.

## ■ REFERENCES

- (1) (a) Cram, D. J.; Cram, J. M. *Container Molecules and Their Guests (Monographs in Supramolecular Chemistry)*; Stoddart, J. F., Ed.; Royal Society of Chemistry: Cambridge, 1994; Vol. 4. (b) Collet, A. In *Comprehensive Supramolecular Chemistry*; Atwood, J. L., Davis, J. E. D., MacNicol, D. D., Vögtle, F., Eds.; Pergamon Press: New York, 1996; Vol. 2, Chapter 11, pp 325–365. (c) Caulder, D. L.; Raymond, K. N. *Acc. Chem. Res.* **1999**, 32, 975–982. (d) Jasat, A.; Sherman, J. C. *Chem. Rev.* **1999**, 99, 931–967. (e) Warmuth, R.; Yoon, J. *Acc. Chem. Res.* **2001**, 34, 95–105. (f) Fujita, M.; Umemoto, K.; Yoshizawa, M.; Fujita, N.; Kusakawa, T.; Biradha, K. *Chem. Commun.* **2001**, 509–518. (g) Rebek, J., Jr. *Angew. Chem., Int. Ed.* **2005**, 44, 2068–2078. (h) Brotin, T.; Dutasta, J. P. *Chem. Rev.* **2009**, 109, 88–130.
- (2) (a) Brotin, T.; Cavagnat, D.; Dutasta, J. P.; Buffeteau, T. *J. Am. Chem. Soc.* **2006**, 128, 5533–5540. (b) Cavagnat, D.; Buffeteau, T.; Brotin, T. *J. Org. Chem.* **2008**, 73, 66–75. (c) Brotin, T.; Cavagnat, D.; Buffeteau, T. *J. Phys. Chem. A* **2008**, 112, 8464–8470. (d) Bouchet, A.; Brotin, T.; Cavagnat, D.; Buffeteau, T. *Chem.—Eur. J.* **2010**, 16, 4507–4518. (e) Bouchet, A.; Brotin, T.; Linares, M.; Agren, H.; Cavagnat, D.; Buffeteau, T. *J. Org. Chem.* **2011**, 76, 1372–1383.
- (3) (a) Canceill, J.; Lacombe, L.; Collet, A. *J. Am. Chem. Soc.* **1985**, 107, 6993–6996. (b) Soulard, P.; Asselin, P.; Cuisset, A.; Aviles Moreno, J. R.; Huet, T. R.; Petitprez, D.; Demaison, J.; Freedman, T. B.; Cao, X.; Nafie, L. A.; Crassous, J. *Phys. Chem. Chem. Phys.* **2006**, 8, 79–92.
- (4) Bouchet, A.; Brotin, T.; Linares, M.; Agren, H.; Cavagnat, D.; Buffeteau, T. *J. Org. Chem.* **2011**, 76, 4178–4181.
- (5) Canceill, J.; Lacombe, L.; Collet, A. *J. Chem. Soc., Chem. Commun.* **1987**, 219–221.
- (6) (a) Darzac, M.; Brotin, T.; Bouchu, D.; Dutasta, J. P. *Chem. Commun.* **2002**, 48–49. (b) Darzac, M.; Brotin, T.; Rousset-Azrel, L.; Bouchu, D.; Dutasta, J. P. *New J. Chem.* **2004**, 28, 502–512.
- (7) Brotin, T.; Barbe, R.; Darzac, M.; Dutasta, J. P. *Chem.—Eur. J.* **2003**, 9, 5784–5792.
- (8) (a) IUPAC-IUB Committee on Biochemistry Nomenclature. *J. Org. Chem.* **1970**, 35, 2849–2867 (IUPAC tentative rules for the nomenclature of organic chemistry. Section E. Fundamental stereochemistry). (b) Collet, A.; Gabard, G.; Jacques, J.; Césario, M.; Guilhem, J.; Pascard, C. *J. Chem. Soc., Perkin Trans. 1* **1981**, 1630–1638.
- (9) Huber, J. G.; Brotin, T.; Dubois, L.; Desvaux, H.; Dutasta, J. P.; Berthault, P. *J. Am. Chem. Soc.* **2006**, 128, 6239–6246.
- (10) Mough, S. T.; Goeltz, J. C.; Holman, K. T. *Angew. Chem., Int. Ed.* **2004**, 43, 5631–5635.
- (11) Hill, P. A.; Wei, Q.; Troxler, T.; Dmochowski, I. J. *J. Am. Chem. Soc.* **2009**, 131, 3069–3077.
- (12) Taratula, O.; Hill, P. A.; Khan, N. S.; Carroll, P. J.; Dmochowski, I. J. *Nat. Commun.* **2010**, 1, 1–7.
- (13) Zhao, Y. H.; Abraham, M. H.; Zissimos, A. M. *J. Org. Chem.* **2003**, 68, 7368–7373.
- (14) “Empty” means that cryptophane is not complexed by a guest molecule, but it is clear that water molecules (solvent) are reversibly exchanging with the cryptophane cavity (sometimes occupied, sometimes not). Moreover, we cannot exclude the presence of dissolved gas

(O<sub>2</sub>, N<sub>2</sub>, etc.) inside the cryptophane cavities because no vacuum treatment has been performed.

(15) (a) Holzwarth, G.; Chabay, I. *J. Chem. Phys.* **1972**, *57*, 1632–1635. (b) Tinoco, I. *Radiat. Res.* **1963**, *20*, 133–139.

(16) (a) Buffeteau, T.; Ducasse, L.; Brizard, A.; Huc, I.; Oda, R. *J. Phys. Chem. A* **2004**, *108*, 4080–4086. (b) Brizard, A.; Berthier, D.; Aimé, C.; Buffeteau, T.; Cavagnat, D.; Ducasse, L.; Huc, I.; Oda, R. *Chirality* **2009**, *21*, S153–S162.

(17) These values correspond to the average conformation of the three linkers over all the steps of dynamics.

(18) Buffeteau, T.; Lagugné-Labarthe, F.; Sourrisseau, C. *Appl. Spectrosc.* **2005**, *59*, 732–745.

(19) Nafie, L. A.; Vidrine, D. W. In *Fourier Transform Infrared Spectroscopy*; Ferraro, J. R., Basile, L. J., Eds.; Academic Press: New York, 1982; Vol. 3, pp 83–123.

(20) Ponder, J. W. *TINKER, Ver. 5.1*; 2010; <http://dasher.wustl.edu/tinker>

(21) (a) Jorgensen, W. L.; Maxwell, D. S.; Tirado-Rives, J. *J. Am. Chem. Soc.* **1996**, *118*, 11225–11236. (b) Maxwell, D. S.; Tirado-Rives, J.; Jorgensen, W. L. *J. Comput. Chem.* **1995**, *16*, 984–1010. (c) Jorgensen, W. L.; McDonald, N. A. *THEOCHEM* **1998**, *424*, 145–155. (d) McDonald, N. A.; Jorgensen, W. L. *J. Phys. Chem. B* **1998**, *102*, 8049–8059. (e) Rizzo, R. C.; Jorgensen, W. L. *J. Am. Chem. Soc.* **1999**, *121*, 4827–4836. (f) Price, M. L. P.; Ostrovsky, D.; Jorgensen, W. L. *J. Comput. Chem.* **2001**, *22*, 1340–1352.

(22) Berendsen, H. J. C.; Postma, J. P. M.; van Gunsteren, W. F.; DiNola, A.; Haak, J. R. *J. Chem. Phys.* **1984**, *81*, 3684–3690.

(23) Frisch, M. J. et al. *Gaussian 03, revision B.04*, Gaussian Inc., Pittsburgh, PA, 2003.